J Electroceram (2011) 26:37–43
DOI 10.1007/s10832-010-9625-4

Lead-free Bi-based complex perovskite nanowires: Sol–gel-hydrothermal processing and the densification behavior

Yu-Dong Hou · Lei Hou · Jing-Li Zhao · Man-Kang Zhu · Hui Yan

Received: 8 April 2010 / Accepted: 20 October 2010 / Published online: 4 November 2010

Abstract One dimensional ferroelectric nanostructure is noteworthy for their size-dependent dielectric, piezoelectric, and electro-optic properties with corresponding applications in smart devices such as transducers, actuators, and high-k dielectrics at the nanoscale. Due to their extremely small size and anisotropy, the control of nucleation and growth of one dimensional nanostructure materials is still a big challenge. Sol–gel-hydrothermal chemistry combines both the merits of sol–gel and hydrothermal technique, which offers a very useful tool for low-temperature synthesis of the ferroelectric nanowires. In this paper, we will review recent works devoted to the synthesis of Bi-based complex perovskite nanowires, i.e. $Na_{0.5}Bi_{0.5}TiO_3$, $K_{0.5}Bi_{0.5}TiO_3$, $(K_{0.5}Bi_{0.5})_{0.4}Ba_{0.6}TiO_3$ and $(Na_{0.8}\ K_{0.2})_{0.5}Bi_{0.5}TiO_3$ systems. We will focus on the formation mechanism and morphology evolution of nanowires prepared in sol–gel-hydrothermal process. Moreover, due to the good sinterability of the nanowires, the high-densified single-phase ceramic can be fabricated even by a conventional sintering process.

Keywords Perovskites · Grain growth · Sol–gel processes · Calcination · Hydrothermal

1 Introduction

Ferroelectric materials are characterized by a switchable macroscopic polarization, which have drawn extensive attention due to their applications in nonvolatile memories, micro-electromechanical systems, nonlinear optics, and sensors [1, 2]. However, at the nanoscale, the ferroelectric structure will exhibit quite different properties from the bulk materials. For example, the ferroelectric properties, including the Curie temperature, mean polarization, area of hysteresis loop, coercive electric field, piezoelectric strain and remnant polarization, will become size dependent. Recently, many theoretical calculations of ferroelectrics with lower dimensionality provide insights not only into how ferroelectric properties of nanowires vary with the size, but also into practical applications, such as how to select a suitable size of nanowires to get the best performance at different temperatures. From the industrial viewpoints, the ferroelectric nanowires have promising applications in miniaturizing piezoelectric transducers and actuators, ultrasonic devices, medical imaging detectors, and using as ferroelectric memories [3–8]. Therefore, the synthesis of ferroelectric nanowires is of great interest not only from a fundamental point of view but also for future applications. It is important to note that nanowires also show supersinterability, which favored to obtain a well-densified single-phase ceramic, specifically for oxides containing high volatility element such as potassium, sodium, etc. Thus, it is of great significance to investigate the fabrication as well as the physical and electrical properties of one dimensional ferroelectric nanowires and ceramics before and after sintering.

Most technological important ferroelectrics are oxides with a perovskite structure. At present, lead zirconate titanate (PZT) based perovskite ceramics are the most widely used in electronic devices due to their high piezoelectric performance [9, 10]. However, the pollutant of toxic lead during the fabrication and waste of products cause a crucial environmental problem. Therefore, there is

Y.-D. Hou (✉) · L. Hou · J.-L. Zhao · M.-K. Zhu · H. Yan
Department of Materials Science and Engineering,
Beijing University of Technology,
Beijing 100124, China
e-mail: ydhou@bjut.edu.cn

an increasing strong demand to develop lead-free piezoelectric ceramics against PZT based compounds [11–13]. For searching the new lead-free substitute, it is important to clarify the feature of Pb element firstly. It is well-known that Pb^{2+} has the special electronic structure of [Xe] $4f^{14}5d^{10}6s^2$. The lone pairs of $6S^2$ are paired by their antiparallel spin in a filled subshell, which formed a dumbbell-like extrusion of the electron density on one side of the ion. This configuration can increase the hybridization strongly with the O 2p states and reduce the distance between the lead ion and one oxygen ion, therefore resulting in the enhancement of the ferroelectric distortion. Accordingly, if one considers replacing the Pb ion while retaining the good ferro- and piezoelectric properties, one should contemplate ions that possess a lone electron pair in an outer shell. In the period table of the chemical elements, Tl^{1+} and Bi^{3+} are the neighbors of Pb, which all have the stereochemically active $6s^2$ lone pairs. Tl is virulent, and the toxicity is even stronger than that of lead, while Bi is nontoxic in its oxide forms; indeed, the active ingredient of a popular antacid is bismuth salicylate. Thus, from the atomistic point of view, bismuth-based perovskite compounds seem to be the most likely successors to lead-based piezoelectrics. Recently, a series of materials with the general formula BiMO$_3$ (M = Al, Ga, In and Fe) have been reported to exhibit ferroelectricity [14–18]. Except $BiFeO_3$, all other perovskites with Bi^{3+} at A site are prepared at high pressure and high temperature conditions. However, $BiFeO_3$ is mutiferroic material with weak ferroelectric behavior, and not meets the requirements of piezoelectric devices. Compared with BiMO$_3$, $Na_{0.5}Bi_{0.5}TiO_3$ (NBT) and $K_{0.5}Bi_{0.5}TiO_3$ (KBT) belong to the complex perovskite compounds. Both NBT and KBT have the large ferroelectric and piezoelectricity properties [12, 19], moreover, they can even construct the Morphotropic Phase Boundary (MPB) with other perovskite compounds, which encouraged studies of the bismuth based complex perovskite compounds of NBT, KBT, $(K_{0.5}Bi_{0.5})_{0.4}Ba_{0.6}TiO_3$ (KBT-BT) and $(K_{0.2}Na_{0.8})_{0.5}Bi_{0.5}TiO_3$ (KBT-NBT) as alternatives to PZT ceramics.

Normally, the ferroelectric bismuth based complex perovskite powders are prepared by solid-state reaction using oxides or carbonates as starting materials [20–22]. As the solid-state reactions are generally controlled by slow diffusion mechanisms, high temperatures and long times must be used for the reactions to go to completion, thus resulting in a high agglomeration and inhomogeneous particle size. Therefore, the prepared powders have low reactivity and they are unsuitable for enhancing the electric properties of ceramics for high-performance uses. Sol–gel is a typical chemical method to prepare ferroelectric powders. However, it was regarded as a solid rather than solution process because sol–gel-derived precipitates are amorphous in nature and calcinations in air are inevitable for the formation of the crystalline material [23–28]. The calcinations lead to serious particle agglomeration, grain growth and small surface area, which all decrease the activity of powder. Due to this reason, it is rarely reported that the conventional sol–gel method can be used to prepare high quality free-standing ferroelectric nanowires. Template-assisted synthesis is a widely used method to produce ferroelectric nanowires. In this method, the most commonly used negative templates are porous anodic aluminium oxide (AAO) and track-etched polycarbonate membranes. These templates have one-dimensional (1D) pores or channels in which a sol or an aqueous solution containing the desired components can be incorporated. In the following drying and annealing steps, the solvent evaporates and the material starts to crystallize and densify, forming nanostructures with dimensions precisely controlled by the pore diameter and the pore length of the template [29–31]. However, this complicated route makes it difficult to scale-up. Electrospinning is also a remarkably method for generating nanofibers. This method combined with two conventional techniques such as spinning and sol–gel, and provides a versatile technique for producing ceramic nanofibers with either a solid, porous, or hollow structure. In this process, a viscous solution is injected from a needle orifice in the presence of electric field. When the applied electric field overcomes the surface tension of the liquid, a continuous jet is ejected which upon subsequent solvent. Subsequent drawing and solidification of the jet lead to the formation of uniform, thin fibers [32–34]. Molten salt method (MSS) is a new developed method to prepare ferroelectric nanowires [35–44]. Although the molten salt is introduced as a solvent in the subsequent calcination of the precursors, they can easily be removed from the as prepared products. Two mechanisms, “dissolution–precipitation” and “template formation,” are involved in MSS. Interfacial energies between the constituents and the salt medium itself are important to determine the ultimate product morphology. This method has been successfully used to prepare monosystem nanowires as $K_{0.5}Bi_{0.5}TiO_3$ [35], $NaNbO_3$ [37], $PbTiO_3$ [38] and $BaTiO_3$ [39]. However, due to the difficulties to control the balance of diffusing rates of various cations simultaneously, this method is handicapped to prepare multisystem ferroelectric nanowires [45]. Hydrothermal synthesis allows formation of ceramic powders directly in water and usually at a temperature below 300°C [46–51]. The synthesis is a single step, consisting of treating in an autoclave an aqueous solution or suspension containing the ions of interest. The conditions of hydrothermal reactions can be optimized by varying the chemical process variables, such as reagent concentrations, temperature, pressure, and pH. Normally, a great variety of morphologies can be obtained, which

usually can be controlled by the synthesis parameters. However, because of the interaction between the powder and water during the entire process, it is generally more difficult to control the chemical composition and homogeneity of the resulting powders containing more than one metallic ion.

As a novel technique to prepare oxide powders at moderate condition, the sol–gel-hydrothermal processing represents an alternative to the calcinations for the crystallization of objective compound under mild temperatures. As we known, sol–gel technique is a conventional preparation method, which could realize evenly mixed gelatin, while hydrothermal technique, in which reactions could take place under elevated pressure and moderated temperature, has many advantages over other manufacture techniques, such as morphology, purity, and lowering down the reaction temperature considerately. The sol–gel-hydrothermal method gives a double advantage of both sol–gel and hydrothermal syntheses and became attractive in the last decade for the possibly of producing highly crystallized and well dispersed ceramic powders at relative low temperature [52–55]. In our recent series works, we have found that the sol–gel-hydrothermal method can also be developed to direct generation of ferroelectric nanowires. It should be noted that this method is low cost and the prepared nanowires have the good sinterability, and the electric properties of the derived ceramics were superior to that prepared by solid-state methods. To the best of our knowledge, these works are the initial works to achieve ferroelectric nanowires, expecially the multi-system Bi-based complex perovskite compounds, by a sol–gel-hydrothermal method so far.

2 Sol–gel-hydrothermal processing of Bi-based complex perovskite series nanowires

2.1 Synthesis and microstructure of Bi-based complex perovskite series nanowires

In our laboratory, we have used the sol–gel-hydrothermal technique to prepare Bi-based complex perovskite based series nanowires. As noted, we found it to be a simple, readily scaleable (in terms of grams) chemical reaction without using expensive apparatus. The typical experimental procedures include [55]: (1) sol–gel preparation: according to the stoichiometric ratio of NBT, KBT, KBT-BT and KBT-NBT, the raw materials of bismuth, sodium, potassium and barium in the form of nitrate or acetate were weighted and then introduced into the solution of tetrabutyl titanate in ethanol. In this step, the control of PH value is important to obtain homogeneous sol. Then, the sol was heated at 80°C to produce a dry gel. (2) Hydrothermal treatments: the obtained gel precursor was poured into a Teflon vessel with NaOH addition, and then subjected to hydrothermal treatment at an appropriate temperature under auto-generated pressure. After cooling, the product was filtered, washed with distilled water, and dried at the ambient temperature.

Figure 1 shows the XRD patterns of KBT powders sol–gel-hydrothermally treated at different temperatures [56]. At the low temperature of 100°C, peaks corresponding to perovskite KBT had begun to appear, but the peaks were ill defined due to the low crystallinity of this phase. The well crystallization phases of KBT were obtained for the samples hydrothermally treated at 160°C and above. For comparison, a part of the gel was calcined at different temperature in muffle furnace, and the results are shown in Figure 2. It can be seen clearly that for the normal sol–gel method, until the temperature increased to 650°C, only the pyrochlore phase of $Bi_2Ti_2O_7$ can be detected and there was no trace of KBT perovskite. In order to obtain the pure KBT phase, the temperature as high as 700°C is needed [57]. So, it is a breakthrough that the synthesizing temperature of KBT perovskite in sol–gel-hydrothermal method was decreased more than 500°C compared to that required in the conventional sol–gel technique.

Figure 3(a) and (b) show the images of KBT samples synthesized by the sol–gel-hydrothermal and conventional sol–gel method, respectively. From Figure 3(a), it is observed clearly that the sample synthesized by sol–gel-hydrothermal process demonstrates the morphology of nanowires, which are monodispersed and are not fused to one another. Each nanowire is uniform in width along its entire length, and the median wire diameter and length of KBT nanowire are about 4 and 100 nm, respectively.

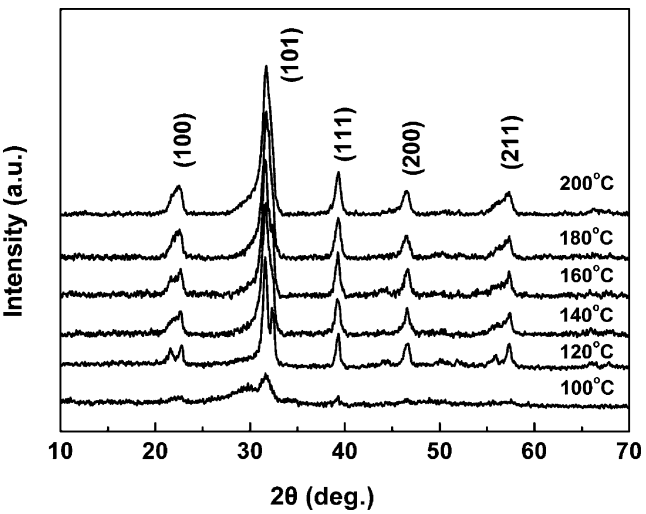

Fig. 1 XRD patterns of KBT powders sol–gel-hydrothermally treated at different temperatures (after [56])

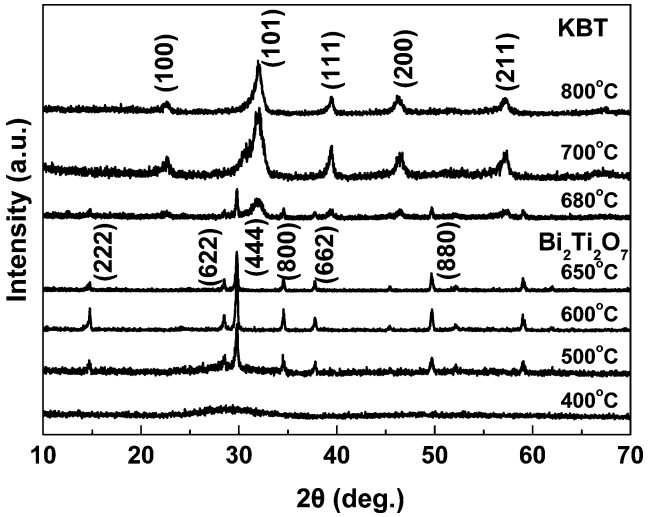

Fig. 2 XRD patterns of the gel calcined at different temperatures (after [56])

Compared with nanowires synthesized by the sol–gel-hydrothermal process, the KBT powders synthesized at 700°C by the conventional sol–gel method consist of the aggregated spherical particles. The detailed morphology characterization can refer to the literatures [55–57]. The above results highlight the particulate morphology of the crystallized KBT particles in the sol–gel-hydrothermal process. This sol–gel-hydrothermal method for preparing KBT nanowires was highly reproducible, and in all cases, similar morphologies were obtained. Figure 3(c) shows the typical TEM photograph of NBT samples synthesized by sol–gel-hydrothermal method [58]. It is observed that like KBT, the sol–gel-hydrothermal derived NBT samples demonstrate a large amount of nano-sized whiskers free from any other particle. Each nanowhisker is uniform in width along its entire length, with nearly uniform diameters of around 20 nm and lengths of around 300 nm. Further, it

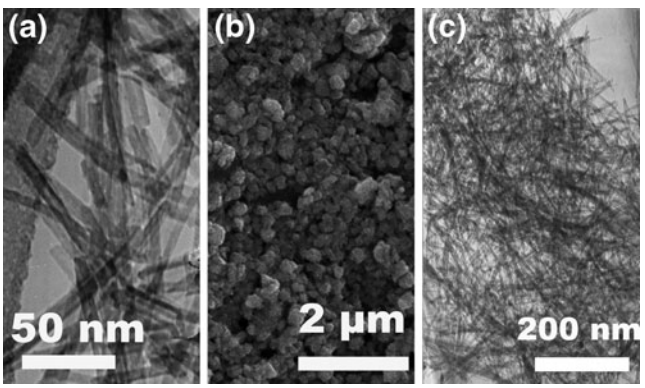

Fig. 3 (**a**) TEM photograph of KBT nanowires synthesized by the sol–gel-hydrothermal method (after [55]), (**b**) SEM photograph of KBT powders synthesized by the conventional sol–gel method (after [56]), (**c**) TEM photograph of NBT nanowires synthesized by the sol–gel-hydrothermal method (after [58])

should be noted that the sol–gel-hydrothermal process can even be extended to the synthesis of binary systems of KBT-BT and KBT-NBT nanowires [59, 60]. In both cases, the synthesis temperatures of pure KBT-BT and KBT-NBT nanowires were below 200°C.

2.2 The formation mechanism of Bi-based complex perovskite series nanowires

Clearly, the planned synthesis of ferroelectric nanowires whose morphology can be controlled at the molecular scale is one of the challenges of molecular chemistry. From this viewpoint, sol–gel-hydrothermal chemistry has a very great future, since it is an ideal link between molecule and nanowire. Recently, a polymer-assisted hydrothermal method has been developed to prepare 1-D nanostructures of oxides. Yang *et. al.* found that the addition of polyacrylate acid (PAA) and polyvinylalcohol (PVA) in hydrothermal process induced the morphology transformation of PZT from cubic shape to orientated nanowhiskers [61]. Hu et al. investigated the anisotropic growth process of $KTa_{0.25}Nb_{0.75}O_3$ (KTN) [62]. They found that when synthesized via a conventional soft chemical route or hydrothermal method, KTN tends to grow uniformly along three major directions, leading to the formation of nano-powders; while using PVA as polymer additives, the [001]-oriented nanorods were observed and the preferred crystallographic orientation of the nanorods can even be controllable by using different types of polymers. In our former work, without using gel precursors, the hydrothermal reaction can only result in the formation of KBT particles with cubic shape [63]. Considering gel precursor is one kind of polymer, it is nature to speculate that the gel precursor containing Ti-O chain played an important role as PVA in the hydrothermal formation of the Bi-based complex perovskite nanowires. Figure 4 shows the schematic diagram of the formation mechanism of ferroelectric nanowires synthesized by sol–gel-hydrothermal method. It is well-known that the growth of nuclei in the calcinations

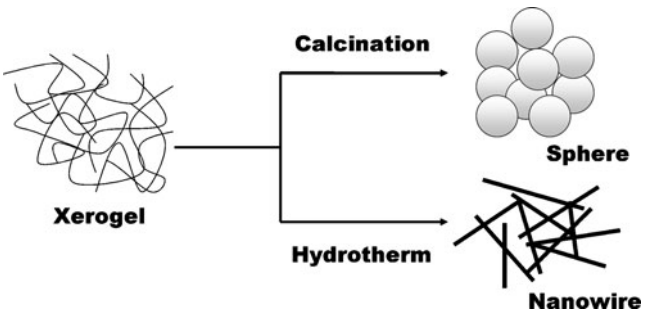

Fig. 4 The schematic diagram of the formation mechanism of Bi-based complex perovskite powders synthesized by sol–gel and sol–gel-hydrothermal methods

of the gels was controlled by the short range diffusion of ions in a limited space; therefore, it is difficult to control the morphology of the final products. Moreover, the high forming temperature of perovskite phase is needed so that the gels have sufficient thermal energy to overcome the atomic/ionic diffusion barriers in the solid reaction. Whereas, in the hydrothermal process, the initial condition of reactant exerts an impact on the crystal nucleation and growth, which is responsible for the morphology of the final products. In sol–gel route, the most important step is the formation of chained nanoclusters by controlling the hydrolysis reactions, during which the molecular precursor is transformed into a highly cross-linked polymer. These chained nanoclusters could serve as the nuclei and nano-reactor during the low temperature hydrothermal treatment, and thus can be used as a soft template to control the morphology of the products [64]. Therefore, nanowires gradually grow freely under the consumption of soft template in aqueous solution. It should be noted that this mechanism is merely a speculated one. The crystal growth is a complex process, which is related to thermodynamics, dynamics, and environments for crystal growth. Thus, more theoretical and experimental works are required to understand this phenomenon.

2.3 Densification of Bi-based complex perovskite series nanowires

The transformation of the gels to nanowires is the domain of molecular chemists, whereas the densification of nanowires to ceramic is mainly the concern of material scientists. It is well known that the morphologies of ceramic powders are quite different from the synthetic procedures, which in turn affect the microstructure and electrical properties of ceramics [65–67]. As the densification is driven by the interfacial energy, it is anticipated that the nanowires are useful in the preparation of dense ceramics by sintering. However, the work related to the sintering behaviors of nanowires has rarely been reported. Recently, we have investigated the sinterability of Bi-based complex perovskite series nanowires in detail [55, 56, 59, 60]. For the four compositions of KBT, NBT, KBT-BT and KBT-NBT, we have found that the sintered pellets made by nanowires showed high bulk density above 96% of theoretical density even by a conventional sintering process. The high densified ceramics have the excellent electrical properties. For example, the sol–gel-hydrothermal derived KBT-NBT ceramics showed d_{33}=156 pC/N, k_p= 0.35, Q_m=165, ε_r=1220 and tanδ=0.022, which are superior to those of previously reported ceramics obtained by other methods [20, 22, 60]. The enhanced electric properties in the sol–gel-hydrothermal-derived ceramics can be attributed to the good sinterability of nanowhiskers, which resulted in the increase in density and a more homogeneous microstructure. As we know that the relative density of a sintered ceramic is directly related to the green density of the pressed pellets, which in turn is highly dependent on the morphology of the precursor oxide powders. The powder synthesized by sol–gel-hydrothermal method gives free-standing nanowires, which have a better packing efficiency and therefore a high green density of above 60% of the theoretical density. In comparison, the green density of the pellets using micro-powders was normally below 50%. It can be hypothesized that the high green density is related to the enhanced plastic deformation of nanowire under the uniaxial pressing. In order to further confirm this speculation, the investigations on the direct in situ plastic deformation process of a nanowire and the related atomic scale mechanism are crucial to provide the quantitative information [68]. In addition, the nature of vacancy defects in these oxide nanowires is another factor facilitating the densification. It is well known that smaller oxide nanowires with high surface to volume ratio should contain more surface oxygen vacancies, which was testified by the x-ray photoelectron spectroscopy (XPS) and photo-luminescence spectroscopy (PL) measurements [69, 70]. Thus, the increased amount of oxygen vacancies would accelerate the transfer of mass and energy between reactants, resulting in the improvement of the sintering behavior.

Figure 5(a) shows the SEM photo of KBT-NBT sintered by conventional method. It is evidenced that the specimen derived from nanowires shows a compact structure with little pores. The mean particle size was about 3 μm. Here, as an extension, other two important sintering methods have also been introduced to densify nanwires: one is the two step sintering method; another is the templated grain growth method (TGG). Two-step sintering exploits the competition between densification and grain growth kinetics in the system of nanoparticles [71–74]. In this process, an elevated temperature in the first stage is one of

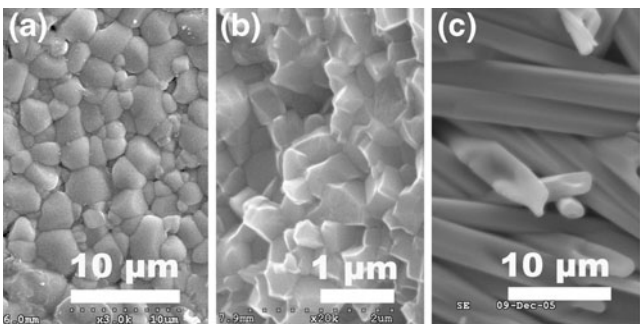

Fig. 5 SEM photographs of Bi-based complex perovskite nanowires densified by different sintering methods: (**a**) KBT-NBT sintered by the conventional method (after [60]), (**b**) KBT sintered by the two step method, (**c**) KBT-BT sintered by the TGG method

the most important conditions. The rate-controlled sintering to the first-step temperature can produce a uniform pore microstructure with less grain growth. Then, the second-step temperature is set lower to enable the driving forces of grain-boundary controlled densification to prevail over boundary-controlled grain growth to achieve densification without grain growth during the final sintering stage. Figure 5(b) shows the SEM photo of KBT specimen sintered by the two step sintering method. The samples show a very homogenous and pore-free structure, which agrees well with the high density above 98% measured for the material. Moreover, it should be noted that the grains were well grown, and the mean particle size was only about 500 nm. In addition, as nanowires have 1-D morphology, they can act as template to construct the textured ceramics. Figure 5(c) shows the SEM photo of KBT-BT specimen sintered by the TGG method. It can be found that the specimens show the oriented alignment of rodlike grains, maintaining partly the initial morphology of nanowires, which is different from their randomly oriented counterparts. Recently, the process of templated grain growth (TGG) has been reported for a variety of materials [75–80]. In this process, the orientation of the textured ceramic is determined by aligning the anisometric grains in a matrix of fine grains. A mixture of the larger "template" nanowires and fine nano-powders with same composition of KBT-BT is oriented during forming and grows preferentially during heating. In our experiment, it was found that the relative size of the matrix and template particles during densification has an important role in the texture development. As the related textured process is out of the topic of this paper and the details will be shown in other paper.

At all, the densification behavior is a difficult and complicated process. In the present time, our knowledge about the densification mechanism of nanowires has been comparatively superficial and further understanding for the mechanism needs much more work. It is hoped that we can achieve this in the coming time.

3 Conclusions

It is clear that ferroelectric nanowires are of fundamental scientific interest due to the size effect and possess a broad range of technological applications as one dimensional nanodevices. In the past few years, vast efforts have been expended in the development of new synthetic approaches for these ferroelectric nanowires. In fact, reproducibly and simultaneously generating control over nanoparticle structure remains an experimental challenge. Recently, through our investigations, it has been shown that sol–gel-hydrothermal chemistry is an efficient tool to prepare Bi-based complex perovskite nanowires. In sol–gel-hydrothermal process, the hydrothermal conditions create a gentle environment to promote the formation of crystalline ferroelectric nanowires at a very low processing temperature. Due to the good sinterability of nanowires prepared by sol–gel-hydrothermal route, the high densified ceramics are easy to prepare by conventional sintering process. The sol–gel-hydrothermal route, without the presence of catalysts and requiring no expensive equipment, will ensure higher purity in the products and greatly reduce the production cost, and thus offer a novel and simple synthetic route for one dimensional nanoscale materials and high quality ceramics.

Acknowledgements The work was partially supported by the National Natural Science Foundation of China (Grant No. 60601020, 51072008), the Natural Science Foundation of Beijing (Grant No. 2102006), and the PHR (IHLB) (Grant No. PHR201008012, PHR201007101).

References

1. R.E. Cohen, Nature **358**, 136 (1992)
2. J.F. Scott, Science **315**, 954 (2007). doi:10.1126/science.1129564
3. Z.Y. Wang, J. Hu, M.F. Yu, Appl. Phys. Lett. **89**, 263119 (2006). doi:10.1063/1.2425047
4. Z.Y. Wang, A.P. Suryavanshi, M.F. Yu, Appl. Phys. Lett. **89**, 082903 (2006). doi:10.1063/1.2338015
5. J.E. Spanier, A.M. Kolpak, J.J. Urban, I. Grinberg, L. Ouyang, W. S. Yun, A.M. Rappe, H.K. Park, Nano Lett. **6**, 735 (2006). doi:10.1021/nl052538e
6. J.W. Hong, D.N. Fang, Appl. Phys. Lett. **92**, 012906 (2008). doi:10.1063/1.2830662
7. G. Pilania, S.P. Alpay, R. Ramprasad, Phys. Rev. B **80**, 014113 (2009). doi:10.1103/PhysRevB.80.014113
8. J.W. Hong, D.N. Fang, J. Appl. Phys. **104**, 064118 (2008). doi:10.1063/1.2982090
9. Y.D. Hou, M.K. Zhu, F. Gao, H. Wang, B. Wang, H. Yan, C.S. Tian, J. Am. Ceram. Soc. **87**, 847 (2004)
10. Y.D. Hou, M.K. Zhu, C.S. Tian, H. Yan, Sens. Actuators A **116**, 455 (2004). doi:10.1016/j.sna.2004.05.012
11. T.R. Shrout, S.J. Zhang, J. Electroceram. **19**, 111 (2007). doi:10.1007/s10832-007-9047-0
12. T. Takenaka, H. Nagata, Y. Hiruma, Jpn. J. Appl. Phys. **47**, 3787 (2008). doi:10.1143/JJAP.47.3787
13. J. Rodel, W. Jo, K.T.P. Seifert, E.M. Anton, T. Granzow, D. Damjanovic, J. Am. Ceram. Soc. **92**, 1153 (2009). doi:10.1111/j.1551-2916.2009.03061.x
14. P. Baettig, C.F. Schelle, R. LeSar, U.V. Waghmare, N.A. Spaldin, Chem. Mater. **17**, 1376 (2005). doi:10.1021/cm0480418
15. A.A. Belik, T. Wuernisha, T. Kamiyama, K. Mori, M. Maie, T. Nagai, Y. Matsui, E.T. Muromachi, Chem. Mater. **18**, 133 (2006). doi:10.1021/cm052020b
16. J. Zylberberg, A.A. Belik, E.T. Muromachi, Z.G. Ye, Chem. Mater. **19**, 6385 (2007). doi:10.1021/cm071830f
17. R.V.K. Mangalam, S.V. Bhat, A. Iyo, Y. Tanaka, A. Sundaresan, C.N.R. Rao, Solid State Commun. **146**, 435 (2008). doi:10.1016/j.ssc.2008.03.039
18. M.M. Kumar, V.R. Palkar, K. Srinivas, S.V. Suryanarayana, Appl. Phys. Lett. **76**, 2764 (2000)
19. S.C. Zhao, G.R. Li, A.L. Ding, T.B. Wang, Q.R. Yin, J. Phys. D **39**, 2277 (2006). doi:10.1088/0022-3727/39/10/042

20. A. Sasaki, T. Chiba, Y. Mamiya, E. Otsuki, Jpn. J. Appl. Phys. **38**, 5564 (1999). doi:10.1143/JJAP.38.5564
21. Y.M. Li, W. Chen, J. Zhou, Q. Xu, H.J. Sun, M.S. Liao, Ceram. Int. **31**, 139 (2005). doi:10.1016/j.ceramint.2004.04.010
22. X.P. Jiang, L.Z. Li, M. Zeng, H.L.W. Chan, Mater. Lett. **60**, 1786 (2006). doi:10.1016/j.matlet.2005.12.021
23. C.Y. Kim, T. Sekino, K. Niihara, J. Am. Ceram. Soc. **86**, 1464 (2003)
24. M.K. Zhu, L. Hou, Y.D. Hou, J.B. Liu, H. Wang, H. Yan, Mater. Chem. Phys. **99**, 329 (2006). doi:10.1016/j.matchemphys.2005.10.031
25. L. Hou, Y.D. Hou, M.K. Zhu, J.L. Tang, J.B. Liu, H. Wang, H. Yan, Mater. Lett. **59**, 197 (2005). doi:10.1016/j.matlet.2004.07.046
26. Y.D. Hou, L. Hou, M.K. Zhu, H. Wang, H. Yan, Mater. Lett. **61**, 3371 (2007). doi:10.1016/j.matlet.2006.11.065
27. C. Wang, Y.D. Hou, H.Y. Ge, M.K. Zhu, H. Wang, H. Yan, J. Cryst. Growth **310**, 4635 (2008). doi:10.1016/j.jcrysgro.2008.08.042
28. C. Wang, Y.D. Hou, H.Y. Ge, M.K. Zhu, H. Yan, J. Eur. Ceram. Soc. **29**, 2589 (2009). doi:10.1016/j.jeurceramsoc.2009.02.012
29. P.M. Rorvik, K. Tadanaga, M. Tatsumisago, T. Grande, M.A. Einarsrud, J. Eur. Ceram. Soc. **29**, 2575 (2009). doi:10.1016/j.jeurceramsoc.2009.02.004
30. X.Y. Zhang, X. Zhao, C.W. Lai, J. Wang, X.G. Tang, J.Y. Dai, Appl. Phys. Lett. **85**, 4190 (2004). doi:10.1063/1.1814427
31. S. Singh, S.B. Krupanidhi, Phys. Lett. A **367**, 356 (2007). doi:10.1016/j.physleta.2006.12.079
32. C. Bae, H. Yoo, S. Kim, K. Lee, J. Kim, M.M. Sung, H. Shin, Chem. Mater. **20**, 756 (2008). doi:10.1021/cm702138c
33. D. Li, J.T. McCann, Y.N. Xia, M. Marquez, J. Am. Ceram. Soc. **89**, 1861 (2006). doi:10.1111/j.1551-2916.2006.00989.x
34. R. Ramaseshan, S. Sundarrajan, R. Jose, S. Ramakrishna, J. Appl. Phys. **102**, 111101 (2007). doi:10.1063/1.2815499
35. J.F. Yang, Y.D. Hou, C. Wang, M.K. Zhu, H. Yan, Appl. Phys. Lett. **91**, 023118 (2007). doi:10.1063/1.2754366
36. H. Deng, Y.C. Qiu, S.H. Yang, J. Mater. Chem. **19**, 976 (2009). doi:10.1039/b815698k
37. C.Y. Xu, L. Zhen, R. Yang, Z.L. Wang, J. Am. Chem. Soc. **129**, 15444 (2007). doi:10.1021/ja077251t
38. Z.Y. Cai, X.R. Xing, R.B. Yu, X.Y. Sun, G.R. Liu, Inorg. Chem. **46**, 7423 (2007). doi:10.1021/ic700966n
39. Y.B. Mao, S. Banerjee, S.S. Wong, J. Am. Chem. Soc. **125**, 15718 (2003). doi:10.1021/ja038192w
40. Y.B. Mao, T.J. Park, F. Zhang, H.J. Zhou, S.S. Wong, Small **3**, 1122 (2007). doi:10.1002/smll.200700048
41. H.Y. Ge, Y.D. Hou, C. Wang, M.K. Zhu, H. Yan, Jpn. J. Appl. Phys. **48**, 041405 (2009). doi:10.1143/JJAP.48.041405
42. Y.B. Mao, T.J. Park, S.S. Wong, Chem. Commun. **46**, 5721 (2005). doi:10.1039/b509960a
43. M.H. Zhang, H.Q. Fan, L. Chen, C. Yang, J. Alloys Compd. **476**, 847 (2009). doi:10.1016/j.jallcom.2008.09.124
44. W.E. Lee, D.D. Jayaseelan, S. Zhang, J. Eur. Ceram. Soc. **28**, 1517 (2008). doi:10.1016/j.jeurceramsoc.2007.12.010
45. J.T. Zeng, K.W. Kwok, H.L.W. Chan, Mater. Lett. **61**, 409 (2007). doi:10.1016/j.matlet.2006.04.083
46. P. Pinceloup, C. Courtois, A. Leriche, B. Thierry, J. Am. Ceram. Soc. **82**, 3049 (1999)
47. E.W. Shi, C.T. Xia, W.Z. Zhong, B.G. Wang, C.D. Feng, J. Am. Ceram. Soc. **80**, 1567 (1997)
48. M.M. Lencka, M. Oledzka, R.E. Riman, Chem. Mater. **12**, 1323 (2000). doi:10.1021/cm9906654
49. Y.J. Ma, J.H. Cho, Y.H. Lee, B.I. Kim, Mater. Chem. Phys. **98**, 5 (2006). doi:10.1016/j.matchemphys.2004.09.045
50. X.Z. Jing, Y.X. Li, Q.R. Yin, Mater. Sci. Eng. B **99**, 506 (2003). doi:10.1016/S0921-5107(02)00515-9
51. X.L. Chen, H.Q. Fan, L.J. Liu, J. Cryst. Growth **284**, 434 (2005)
52. Z.J. Li, B. Hou, Y. Xu, D. Wu, Y.H. Sun, W. Hu, F. Deng, J. Solid State Chem. **178**, 1395 (2005). doi:10.1016/j.jssc.2004.12.034
53. H. Wang, L. Wang, J.B. Liu, B. Wang, H. Yan, Mater. Sci. Eng. B **99**, 495 (2003)
54. Z.Q. Song, S.B. Wang, W. Yang, M. Li, H. Wang, H. Yan, Mater. Sci. Eng. B **113**, 121 (2004). doi:doi:10.1016/j.mseb.2004.06.002
55. L. Hou, Y.D. Hou, X.M. Song, M.K. Zhu, H. Wang, H. Yan, Mater. Res. Bull. **41**, 1330 (2006). doi:10.1016/j.materresbull.2005.12.010
56. Y.D. Hou, L. Hou, S.Y. Huang, M.K. Zhu, H. Wang, H. Yan, Solid State Commun. **137**, 658 (2006). doi:10.1016/j.ssc.2006.01.023
57. Y.D. Hou, M.K. Zhu, L. Hou, J.B. Liu, J.L. Tang, H. Wang, H. Yan, J. Cryst. Growth **273**, 500 (2005). doi:10.1016/j.jcrysgro.2004.09.055
58. J.B. Liu, H. Wang, Y.D. Hou, M.K. Zhu, H. Yan, M. Yoshimura, Nanotechnology **15**, 777 (2004). doi:10.1088/0957-4484/15/7/010
59. Y.D. Hou, L. Hou, M.K. Zhu, H. Yan, Appl. Phys. Lett. **89**, 243114 (2006). doi:10.1063/1.2405881
60. Y.D. Hou, L. Hou, T.T. Zhang, M.K. Zhu, H. Wang, H. Yan, J. Am. Ceram. Soc. **90**, 1738 (2007). doi:10.1111/j.1551-2916.2007.01657.x
61. X.Q. Yang, Y.N. Zhao, Y. Yang, Z.H. Dong, Mater. Lett. **61**, 3462 (2007). doi:10.1016/j.matlet.2006.11.088
62. Y.M. Hu, H.S. Gu, D. Zhou, Z. Wang, H.L.W. Chan, Y. Wang, J. Am. Ceram. Soc. **93**, 609 (2010). doi:10.1111/j.1551-2916.2009.03461.x
63. L. Hou, Y.D. Hou, X.M. Song, M.K. Zhu, H. Wang, H. Yan, Chin. J. Inorg. Chem. **22**, 563 (2006)
64. J.H. Liang, C. Peng, X. Wang, X. Zheng, R.J. Wang, X.P. Qiu, C. W. Nan, Y.D. Li, Inorg. Chem. **44**, 9405 (2005). doi:10.1021/ic048237+
65. A. Banerjee, S. Bose, Chem. Mater. **16**, 5610 (2004). doi:10.1021/cm0490423
66. H.Y. Ge, Y.D. Hou, M.K. Zhu, H. Wang, H. Yan, Chem. Commun. **41**, 5137 (2008). doi:10.1039/b810342a
67. S.J. Qiu, H.Q. Fan, C. Yang, J. Chen, J. Am. Ceram. Soc. **90**, 3293 (2007). doi:10.1111/j.1551-2916.2007.01852.x
68. X.D. Han, Z. Zhang, Z.L. Wang, Nano Brief Rep. Rev. **2**, 249 (2007)
69. Y.M. Hu, H.S. Gu, X.C. Sun, J. You, J. Wang, Appl. Phys. Lett. **88**, 193120 (2006). doi:10.1063/1.2203736
70. H.S. Gu, Y.M. Hu, J. You, Z.L. Hu, Y. Yuan, T.J. Zhang, J. Appl. Phys. **101**, 024319 (2007). doi:10.1063/1.2430768
71. A. Polotai, K. Breece, E. Dickey, C. Randallw, A. Ragulya, J. Am. Ceram. Soc. **88**, 3008 (2005). doi:10.1111/j.1551-2916.2005.00552.x
72. T. Karaki, K. Yan, M. Adachi, Jpn. J. Appl. Phys. **46**, 7035 (2007). doi:10.1143/JJAP.46.7035
73. T.T. Zou, X.H. Wang, W. Zhao, L.T. Li, J. Am. Ceram. Soc. **91**, 121 (2008). doi:10.1111/j.1551-2916.2007.01903.x
74. T.T. Zou, X.H. Wang, H. Wang, C.F. Zhong, L.T. Li, I.W. Chen, Appl. Phys. Lett. **93**, 192913 (2008). doi:10.1063/1.2995861
75. Y. Saito, H. Takao, T. Tani, T. Nonoyama, K. Takatori, T. Homma, T. Nagaya, M. Nakamura, Nature **432**, 84 (2004). doi:10.1038/nature03028
76. T. Kimura, T. Takahashi, T. Tani, Y. Saito, J. Am. Ceram. Soc. **87**, 1424 (2004)
77. S.H. Hong, S.T. McKinstry, G.L. Messing, J. Am. Ceram. Soc. **83**, 113 (2000)
78. C. Duran, S.T. McKinstry, G.L. Messing, J. Am. Ceram. Soc. **83**, 2203 (2000)
79. J.L. Jones, B.J. Iverson, K.J. Bowman, J. Am. Ceram. Soc. **90**, 2297 (2007). doi:10.1111/j.1551-2916.2007.01820.x
80. J.A. Horn, S.C. Zhang, U. Selvaraj, G.L. Messing, S.T. McKinstry, J. Am. Ceram. Soc. **82**, 921 (1999)